Video Article

# Imaging Plasma Membrane Deformations With pTIRFM

Daniel R. Passmore[1], Tejeshwar C. Rao[1], Andrew R. Peleman[1], Arun Anantharam[1]

[1]Department of Biological Sciences, Wayne State University

Correspondence to: Arun Anantharam at Anantharam@wayne.edu

URL: https://www.jove.com/video/51334
DOI: doi:10.3791/51334

Keywords: Biochemistry, Issue 86, Chromaffin Cells, Lipid Bilayers, Microscopy, Fluorescence, Polarization, Exocytosis, membrane, TIRF, pTIRF, chromaffin, polarization, vesicle

Date Published: 4/2/2014

Citation: Passmore, D.R., Rao, T.C., Peleman, A.R., Anantharam, A. Imaging Plasma Membrane Deformations With pTIRFM. *J. Vis. Exp.* (86), e51334, doi:10.3791/51334 (2014).

## Abstract

To gain novel insights into the dynamics of exocytosis, our group focuses on the changes in lipid bilayer shape that must be precisely regulated during the fusion of vesicle and plasma membranes. These rapid and localized changes are achieved by dynamic interactions between lipids and specialized proteins that control membrane curvature. The absence of such interactions would not only have devastating consequences for vesicle fusion, but a host of other cellular functions that involve control of membrane shape. In recent years, the identity of a number of proteins with membrane-shaping properties has been determined. What remains missing is a roadmap of when, where, and how they act as fusion and content release progress.

Our understanding of the molecular events that enable membrane remodeling has historically been limited by a lack of analytical methods that are sensitive to membrane curvature or have the temporal resolution to track rapid changes. PTIRFM satisfies both of these criteria. We discuss how pTIRFM is implemented to visualize and interpret rapid, submicron changes in the orientation of chromaffin cell membranes during dense core vesicle (DCV) fusion. The chromaffin cells we use are isolated from bovine adrenal glands. The membrane is stained with a lipophilic carbocyanine dye,1,1'-dioctadecyl-3,3,3',3'-tetramethylindodicarbocyanine, 4-chlorobenzenesulfonate, or diD. DiD intercalates in the membrane plane with a "fixed" orientation and is therefore sensitive to the polarization of the evanescent field. The diD-stained cell membrane is sequentially excited with orthogonal polarizations of a 561 nm laser (p-pol, s-pol). A 488 nm laser is used to visualize vesicle constituents and time the moment of fusion. Exocytosis is triggered by locally perfusing cells with a depolarizing KCl solution. Analysis is performed offline using custom-written software to understand how diD emission intensity changes relate to fusion pore dilation.

## Video Link

The video component of this article can be found at https://www.jove.com/video/51334/

## Introduction

The proper execution of exocytosis requires extreme changes in membrane bilayer shape to be precisely orchestrated. Prior to fusion, local bending of the plasma membrane under the granule occurs, in part to reduce the energy barrier for interaction of bilayers. Later, as membranes merge, areas of high curvature are generated and must be stabilized. Finally, fused membranes must be bent out of their initial shape to expand the fusion pore and enable content release[1]. Because membranes alone are unlikely to undergo such dramatic and coordinated changes, proteins are necessary to mediate events. But how they act to influence changes in membrane topology during the fusion process remains very much an open question.

Excellent *in vitro* models exist to visualize membrane curvature. The use of negative-stain EM, for instance, has been important for shaping current molecular models for the actions of two major trafficking proteins - synaptotagmin and dynamin (for reviews, see Chapman[2] and Henshaw[3]). Most real-time assays of exocytosis do not detect curvature directly. Instead, curvature is inferred from assays that report on the kinetics of lumenal cargo release[4-8] or changes in membrane area[9-11]. PTIRFM bridges the gap between *in vivo* and *in vitro* studies by enabling direct, real-time measurements of changes in membrane micromorphology.

PTIRFM, in a nonimaging mode, was pioneered by Axelrod and colleagues to measure the orientation of NPD-PE incorporated within a model membrane[12]. The technique was then applied to visualize dynamic changes in living cells labeled with dil and FM1-43[13-18]. In pTIRFM, two evanescent field polarizations are used to sequentially excite a membrane-embedded probe: p-polarization (in the plane of incidence) and s-polarization (perpendicular to the plane of incidence). Prior to imaging, the probe - in this case, diD - is briefly added to the extracellular medium and is allowed to intercalate in the plasma membranes of the cells to be studied. In regions where the membrane is nonparallel to the coverglass (as in a membrane ruffle or indentation), the diD will also be nonparallel. Therefore, such regions will be excitable by the p-pol beam. The p-pol beam will less effectively excite diD in membrane regions that are mostly parallel to the coverglass. Pixel-to-pixel ratio images (*P/S*) reporting on the emission from sequential p- and s-pol excitation of diD will therefore specifically highlight regions of membrane deformation. In theory, the *P/S* ratio images are sensitive to even small angles of plasma membrane deviation from the coverglass, with the amplitude of the changes predicted by computer simulations[18]. *P/S* images are also independent of fluorophore distance from the coverglass surface and local fluorophore concentration. Local fluorophore concentration is instead provided by images reporting on the pixel-to-pixel sum of the P emission and 2 times

the S emission (*P+2S*). The *P+2S* measurement is sensitive to the precise geometry of the indentation, with some, little, or no change possible. This can be shown by computer simulations that model transitions of a fusion pore from an early (*i.e.* with a narrow neck) to a later state[16,18]. The *P+2S* of a fused vesicle attached to the plasma membrane via a narrow neck (and with more diD close to the interface) is predicted to be greater, for example, than that of a fused vesicle with a much wider pore (where the diD is within the dimmest part of the evanescent field).

In this article, we discuss how pTIRFM is implemented and utilized to study the rapid, localized changes in membrane shape that occur during fusion pore dilation. While only one application is explicitly discussed, the methods are generalizable to a variety of other cell biological processes that directly or indirectly involve membrane remodeling.

## Protocol

# 1. PTIRF System Setup

The pTIRFM technique is built on an inverted microscope platform. Laser beams are directed through a side illumination port and a nonpolarizing side-facing filter cube, and then focused onto the back focal plane of a 60X 1.49 NA TIRF objective. Two additional lenses (1.6X and 2X) in the emission path between the microscope and EMCCD camera give a final pixel size of approximately 80 nm. Laser beams are guided using software controlled galvanometer mirrors for rapid switching between epi- and total internal reflection (TIR) illumination. The protocol described below assumes that optics for TIRF are already positioned on the air table in the optimum positions for fluorophore excitation and imaging. It describes how polarization optics are added to an existing TIRF microscope set-up to enable imaging of cell membrane deformations. A schematic of our laboratory's optical set-up for generating both TIR and polarization-based TIR is shown in **Figure 1A**. The protocol assumes the use of a 488-nm laser for excitation of fluorescent vesicle proteins and a 561 nm laser for the imaging of the carbocyanine dye, diD.

1. Power on all microscope components, lasers, and computers.
2. Direct a beam from the 488 nm laser to the back focal plane (BFP) of the 1.49 NA lens as illustrated in **Figure 1A**. If the laser beam is focused on the BFP, it will emerge collimated and appear as small well-defined spot on the ceiling directly above the objective.
3. Adjust the X galvanometer mirror (the mirror located in the equivalent sample plane) so that laser beam is moved off-axis and emerges from the objective at progressively steeper angles to the objective normal.
4. Next, verify that TIR is achieved. Add 10 µl of fluorescent microspheres to a 1 ml volume of PSS in a glass-bottom dish. Only fluorescence from microspheres on the bottom of the dish, closest to the TIR interface, should be detected. Detection of floating microspheres indicates that the angle between the incident light and objective normal is insufficient.
   The section below describes the set-up of the optical components necessary for polarization-based imaging.
5. Using the aligned 488 nm beam as a guide, adjust the position of the raw 561 nm laser beam so it is traveling along an identical optical path. The 561 nm laser will be used for imaging of the carbocyanine dye, diD.
6. Insert a diverging lens and mirrors downstream of the 561 nm laser. Using the mirrors, adjust the beam so that it is coaligned with the 488 nm beam and the spot is in focus on the ceiling when the galvanometer mirrors are in the "0" position.
7. Center a quarter-wave plate (QW) in the beam path immediately downstream of the laser aperture. Use a QW which is either achromatic or tuned to the excitation wavelength. A QW will circularly polarize any linearly polarized light which enters at a 45° angle with the optical axis. Some optical components, such as the polarization cubes, have an attenuation bias towards one axis of polarization. The QW may be rotated to compensate for this bias. This adjustment will result in an elliptically polarized beam. A QW is necessary because the laser beam itself is highly linearly polarized (vertically) as it emerges from the aperture.
8. Place a polarization cube (PC1) downstream of the elliptically polarized beam. The polarization cube reflects the vertical (y) component of the electric field and passes the horizontal (x) component. The polarization cube is placed on a small translating stage to facilitate subsequent alignment of polarization beam paths.
9. Use a second polarizing cube (PC2) and mirrors (**Figure 1A**) to recombine the beams.
10. Place a shutter between the first polarization cube (PC1) and the vertical component mirror. Place a second shutter between the horizontal component mirror and second polarization cube (PC2). These shutters are controlled by the imaging software enabling the user to rapidly select between beam polarizations.
11. Use a polarizing filter to verify the electric field orientation in each beam path. A polarizing filter will only allow transmission in line with the filter's axis.
12. Verify that the vertical and horizontal components of the laser beam are aligned with each other and the 488 nm beam. Make adjustments as necessary. The three beams should all be focused on the BFP and emerge collimated from the objective to the same spot on the ceiling. This spot can be marked by an X to facilitate future alignment.
13. Place a drop of immersion oil on the objective. Place the dish containing fluorescent microspheres (see step 4 above) on the objective.
14. Enter TIR by moving the X galvanometer mirror. In TIR, the vertical component of the beam is the s-pol and the horizontal component of the beam is now the p-pol. Adjust the relative intensity between the beams by rotating the QW plate. View each polarized evanescent field with a rhodamine sample, which is predicted to be randomly oriented. Rotate the QW plate to match the average pixel intensities. If necessary, add a neutral density filter in one polarized beam path to attenuate its intensity.

# 2. Chromaffin Cell Isolation

A procedure for isolating healthy chromaffin cells from the calf adrenal gland is provided below. It is adapted from previously published protocols by Wick, Senter, *et al.*[19] and O'Connor, Mahata *et al.*[20] After isolation, cells are electroporated with plasmid(s) of interest using an electroporation system. This system results in 20-30% of cells expressing the desired fluorescent proteins. Typically, 70% of cells survive the electroporation process. Details of the PSS and media components are provided in **Tables 2, 3,** and **4**.

1. Two days before the cell prep, treat 35-mm optical quality glass-bottom (0.17 mm thick) dishes with 1 ml poly-D-lysine (0.1 mg/ml) followed by 1.25 ml bovine collagen. Leave dishes to air dry in tissue culture hood.

2. Obtain bovine adrenal glands from the abattoir. Keep the glands on ice while they are transported back to the lab. The bovine adrenal glands may be encased in a thick layer of fat. Use surgical scissors to remove excess fat and expose the adrenal vein opening. Perfuse the vein with prep-PSS repeatedly until the gland is purged of blood.
3. Next, slowly pipette 2 ml of TH-PSS solution into the vein opening until the gland swells. Incubate the inflated glands at 37 °C for 15 min. Repeat the TH-PSS treatment and incubate again.
4. Cut through the outer adrenal cortex around the edge of the gland with scissors and peel the gland apart to expose the medulla. Use a scalpel to gently scrape and separate the medulla from the cortical tissue.
5. Mince the medulla with a pair of scalpel blades for 5-10 min.
6. A final digestion step is necessary to isolate individual chromaffin cells. Pour the minced cell suspension into a spinner flask. Partially fill the flask with a 2:1 ratio of TH-PSS (30 ml) to TL-PSS (15 ml) and incubate for 30 min at 37 °C while spinning at approximately 100 rpm.
7. Separate the individual chromaffin cells from undigested tissue by filtering through a 400 µm mesh. Collect the filtrate. Centrifuge at 200 x g to pellet the cells, and resuspend in ice cold PSS.
8. Filter the cells through a 250 µm mesh, pellet, and finally resuspend in electroporation buffer (see step 2.9).
9. Count cells using a hemocytometer and prepare for transfection.
10. Transfect cells with the electroporation system according to the manufacturer's recommendations. The precise conditions for electroporation must be determined empirically. Note: The settings which provide the best balance between transfection efficiency and cell survival rate for this preparation of bovine chromaffin cells are 1,100 V, 40 msec, and 1 pulse. We estimate that with these conditions, 20-30% of cells are transfected. About 30% of the cells do not survive the electroporation process.
11. Plate cells gently on poly-D-lysine and collagen treated dishes in 1 ml of warmed electroporating media.
12. Place dishes in a 37 °C incubator (5% $CO_2$). Add 1 ml of 2x antibiotic media to each dish after 6 hr. Change the media to normal media the next day.
13. Chromaffin cells are typically imaged 2-5 days after electroporation.

## 3. pTIRF Image Acquisition

1. Power on imaging system and start acquisition software.
2. Verify that lasers are aligned. Check evanescent field profile using microspheres.
3. Prepare the global and local perfusion system. Clean solution reservoirs with filtered deionized $H_2O$ and fill with basal and stimulating PSS solutions.
4. Before imaging chromaffin cells, verify that the p-pol and s-pol excitations illuminate the same region of the viewing field and that the illumination intensities are roughly equivalent. To do this, fill a glass-bottom dish with 2 ml of PSS containing rhodamine at a final concentration of 10 mM. Sequentially excite the rhodamine sample with p-pol and s-pol light and capture the images. In practice, the P and S emissions from diD are normalized to the mean of the P and S rhodamine emissions. See the Image Analysis and Discussion sections for further details.
5. Now proceed to staining bovine chromaffin cells with diD. Rinse culture media from the dish containing the chromaffin cells and replace with 2 ml of basal-PSS. Add 10 µl of 10 mM diD (diluted in ethanol) directly to the dish containing the cells. Gently agitate dish for 2-10 sec and remove the diD + PSS solution.
6. Wash the dish 3-4x with basal-PSS to remove any residual diD. The cells are now stained and ready to use.
7. Add a drop of immersion oil to the objective. Place dish containing diD-stained chromaffin cells on top of the objective.
8. Viewing the dish either through the objective or on the camera, find a cell which is transfected with the protein of interest and stained with diD. A well-stained cell exhibits a P emission that vividly highlights the edges of the cell; the S emission should be roughly uniform across the cell footprint (*i.e.* the region of the cell that is adhered to the glass and imaged in TIRF).
9. Position the local perfusion needle so that it is roughly 100 µm away from the cell.
10. Focus on the cell membrane and activate the autofocus hardware immediately before cell stimulation/image acquisition.
11. Begin image acquisition. Perfuse cells for 10 sec with a basal solution and then for 60 sec with a depolarizing 56 mM KCl solution. Acquire images while rapidly shuttering between 561 nm p-pol, 561 nm s-pol (to monitor changes in P and S emission of diD) and 488 nm excitation (to image the transfected vesicle probe). Examples of images acquired during experiments are shown in **Figure 2** and **Figure 3**.

## 4. Image Analysis

Calculations for image processing may be performed with ImageJ, but utilizing scripts in a flexible programming language such as IDL or Matlab can greatly increase analysis throughput by automating the task. Two types of images must be calculated to obtain topological information from raw emission images - the *P/S* and *P+2S*. *P/S* reports on local membrane deformations while the *P+2S* sum reports on the total membrane dye in a given region of the field.

1. All images should be background subtracted. Choose an off-cell ROI, measure the average pixel intensity in the ROI, and then subtracting that value from all pixels in the image stack.
2. To calculate *P/S*, divide each "P" emission frame by the subsequent "S" emission frame (pixel-to-pixel). *P/S* varies with the relative intensities of the p- and s-pol excitations, biases in the optical system, and interference fringes. To reduce these effects, normalize the *P/S* ratios from obtained from diD emission to the ratio obtained with a solution containing 10 mM rhodamine[18].
3. Exocytosis of individual DCVs is evident from a sudden change in intensity of a fluorescent vesicle protein, such as Synaptotagmin-1 pHluorin (**Figure 2B**). Determine changes in *P/S* and *P+2S* by averaging the pixels in a 240 nm radius ROI centered over localized increases in the *P/S* ratio at sites of exocytosis. When fusion occurs without an evident increase in *P/S*, the ROI is centered over the region of the fusing DCV.
4. Computer simulations can be performed to interpret *P/S* and *P+2S* membrane intensity changes in terms of simple geometries of a dilating fusion pore. For details of the simulations, please see Anantharam *et al.*[18]

## Representative Results

Conventional and polarized TIRFM imaging techniques are implemented on the same air table. The configuration of the optical elements is similar, with the major difference that the excitation light is polarized (**Figure 1A**). Polarized light preferentially excites fluorophores with absorption dipoles in the polarization direction. Thus, for pTIRFM to be effective at monitoring membrane topological changes, the probe that is used must intercalate in the membrane with a fixed orientation. The fluorescent carbocyanine dyes (diI, diD) intercalate into lipid bilayers in an oriented fashion with transition dipoles in the membrane plane (**Figure 1B**). P-polarized illumination (**Figure 1C**) of diD-labeled membranes selectively excites coverslip-oblique fluorophores (RED in **Figures 1B** and **1D**).

Exuberant membrane labeling of chromaffin cells is achieved after a brief incubation with diD. **Figure 2A** shows an example of a cell membrane that is stained well. A healthy, adherent cell will exhibit distinct differences in P and S emissions. The P emission image shows a brighter cell border with respect to the rest of cell. The S emission image shows roughly uniform fluorescence across the cell footprint. Calculated pixel-to-pixel P/S and P+2S images are sensitive to membrane curvature and dye concentration, respectively. The chromaffin cell shown has also been transfected with Synaptotagmin-1 pHluorin (Syt-1) to label secretory vesicles (**Figure 2B**).

The chromaffin cell is stimulated with 56 mM KCl to depolarize the cell membrane and trigger exocytosis. A number of brightly fluorescent Syt-1 pHluorin spots suddenly become evident as DCVs fuse (**Figure 2B**, right panel). A white box is drawn around one fusion event (**Figure 2B**, right panel). This fusion event is analyzed in **Figures 2C** and **2D**. **Figure 2C** shows frame-by-frame changes in Syt-1-pHluorin, *P/S*, and *P+2S* image intensities. Fluorescence intensity of Syt-1 quickly diminishes as the protein diffuses away from the fusion site (**Figure 2D**). The indentation representing the fused vesicle/plasma membrane complex diminishes at a relatively slower rate (Note graphs in **Figure 2D**). The illustration (**Figure 2E**) depicts one interpretation of these measurements.

The rapid and localized membrane deformations shown in **Figure 2** are a result of stimulus-evoked $Ca^{2+}$ influx. This is shown in **Figure 3A**. A chromaffin cell is transfected with the genetic $Ca^{2+}$ indicator GCaMP5G[21,22] and stimulated with 56 mM KCl. Membrane depolarization causes a significant increase in GCaMP5G fluorescence (**Figures 3A** and **3B**) signifying an increase in subplasmalemmal $Ca^{2+}$ levels. A 30 x 20 pixel region of the cell is selected and frame-by-frame changes in GCaMP5G, *P/S*, and *P+2S* pixel intensities are shown in the images (**Figure 3B**) and graphs (**Figure 3C**). Time "0" designates the frame before a change a *P/S* is evident (*i.e.* the frame before exocytosis). The white arrowheads indicate that the membrane deformation (increase in *P/S*) is accompanied by a decrease in *P+2S* emission. The cytosolic GCaMP5G protein is excluded from the area by the fused DCV. Note also the sudden decrease in GCaMP5G intensity at time 0 in **Figure 3C**, left panel. The long-lived increase in *P/S* and decrease in *P+2S* suggest a fusion pore that dilates slowly (**Figure 3D**).

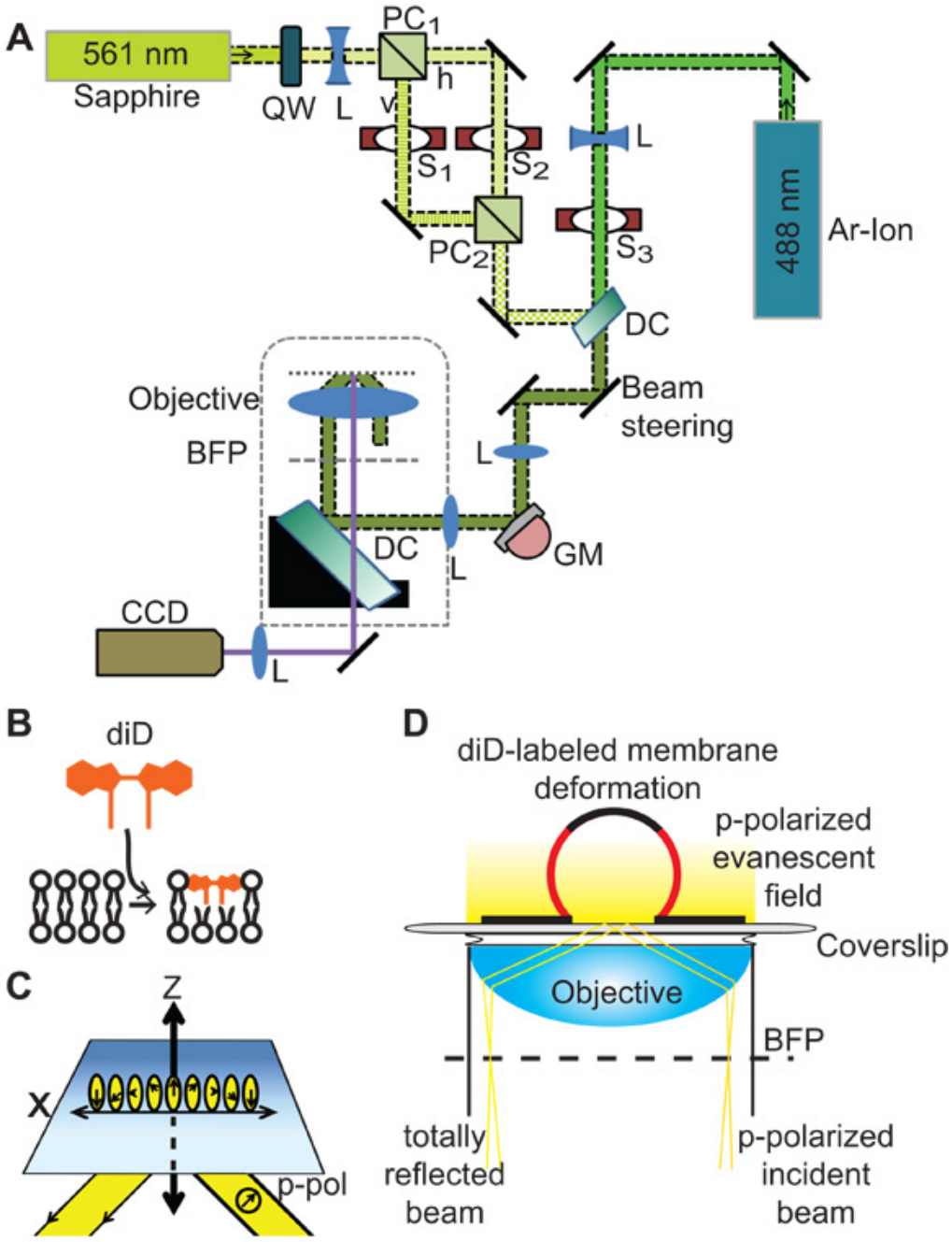


**Figure 1. Illustrations for the pTIRFM technique. A**) A schematic for combining conventional with polarization-based TIRF imaging is shown. A quarter-wave (QW) plate is placed in front of a 561-nm sapphire laser to elliptically polarize the laser beam. A polarizing cube (PC1) is used to separate polarizations into linear vertical (v) and horizontal (h) components. The vertical and horizontal components become the p-pol and s-pol excitation beams, respectively, at the TIR surface. The p-pol and s-pol paths are independently shuttered (S1 and S2). They are recombined with mirrors and a second polarizing cube (PC2). They join the 488 nm beam (also independently shuttered, S3) via a beam steering element consisting of a mirror and nonpolarizing dichroic mirror (DC). Lenses (L) are used to expand and focus the beams. Combined 488-nm and 561-nm beams are steered to a side illumination port of the microscope via galvanometer mirrors (GM). They focus to the back focal plane (BFP) of the objective. Photons emitted from fluorophores are captured on an EMCCD camera connected to a PC. **B**) DiD labeling is performed by briefly incubating cells with the dye and washing repeatedly to remove excess. DiD intercalates in the membrane with its transition dipole moments roughly in the membrane plane. **C**) The incident light polarized in the plane of incidence (p-pol) creates an evanescent field that is predominantly polarized normal to the interface, as shown. **D**) Illumination of a diD-labeled membrane with p-polarized light will selectively excite those fluorophores that are coverglass-oblique (RED). If this were an s-polarized evanescent field, those fluorophores that are parallel to the coverglass would be excited instead (BLACK).

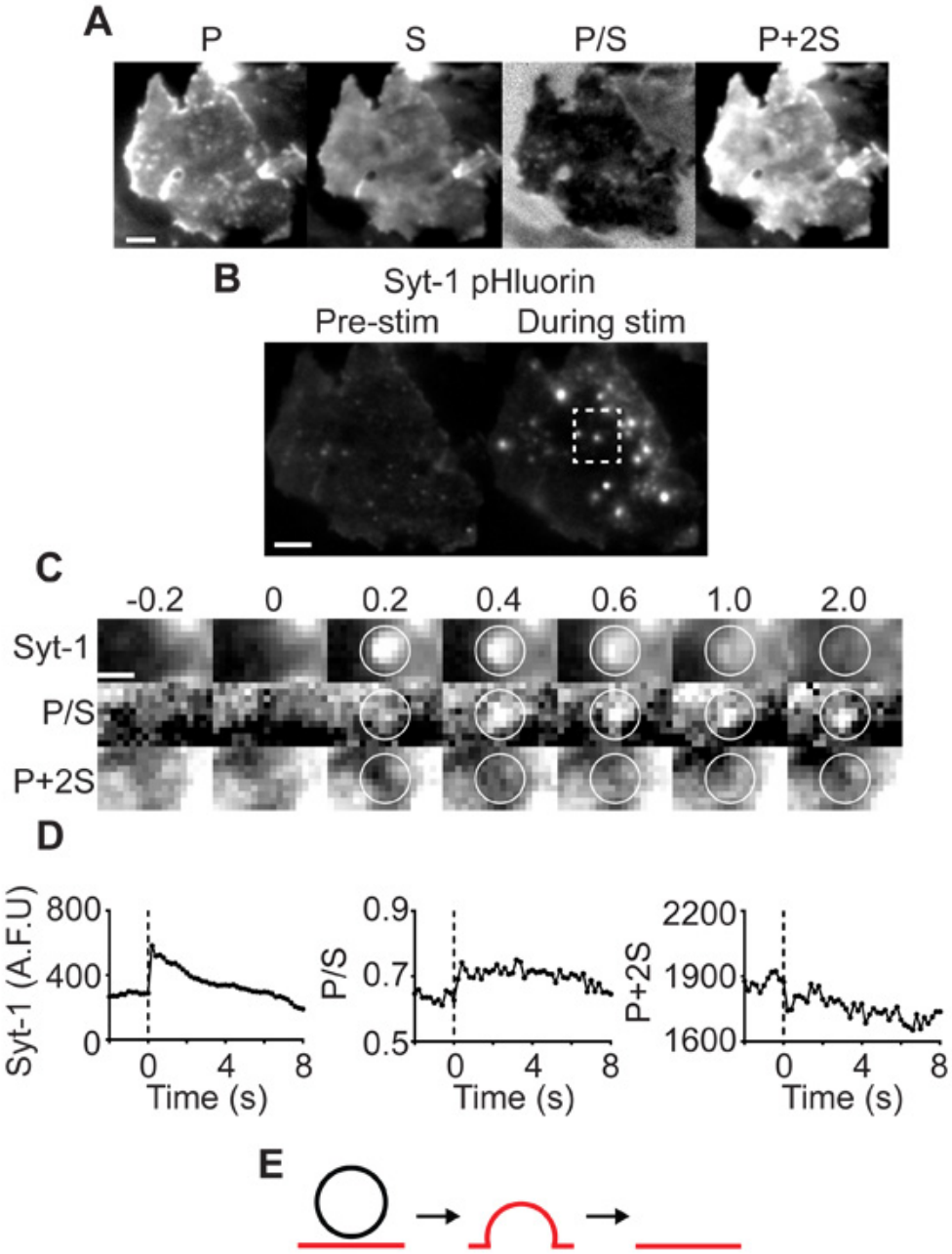


**Figure 2. Monitoring cell membrane deformations with pTIRFM. A**) Raw P and S emission images along with calculated *P/S* and *P+2S* emission images are shown. Scale bar, 3.2 µm. **B**) A chromaffin cell expressing Syt-1 pHluorin is depolarized with KCl. A number of brightly fluorescent spots (right panel) indicate the fusion of individual DCVs. Scale bar, 3.2 µm. **C**) Frame-by-frame images of a fusing Syt-1 pHluorin DCV. Times (above images) are in seconds. Time 0 designates frame before fusion of the DCV. Corresponding *P/S* and *P+2S* emission images are also shown. Scale bar is 1 µm. **D**) Graphs for images in C. Dotted line is at time 0 -- the fusion frame. **E**) One possible interpretation of the results in **C** and **D** is shown. Please click here to view a larger version of this figure.

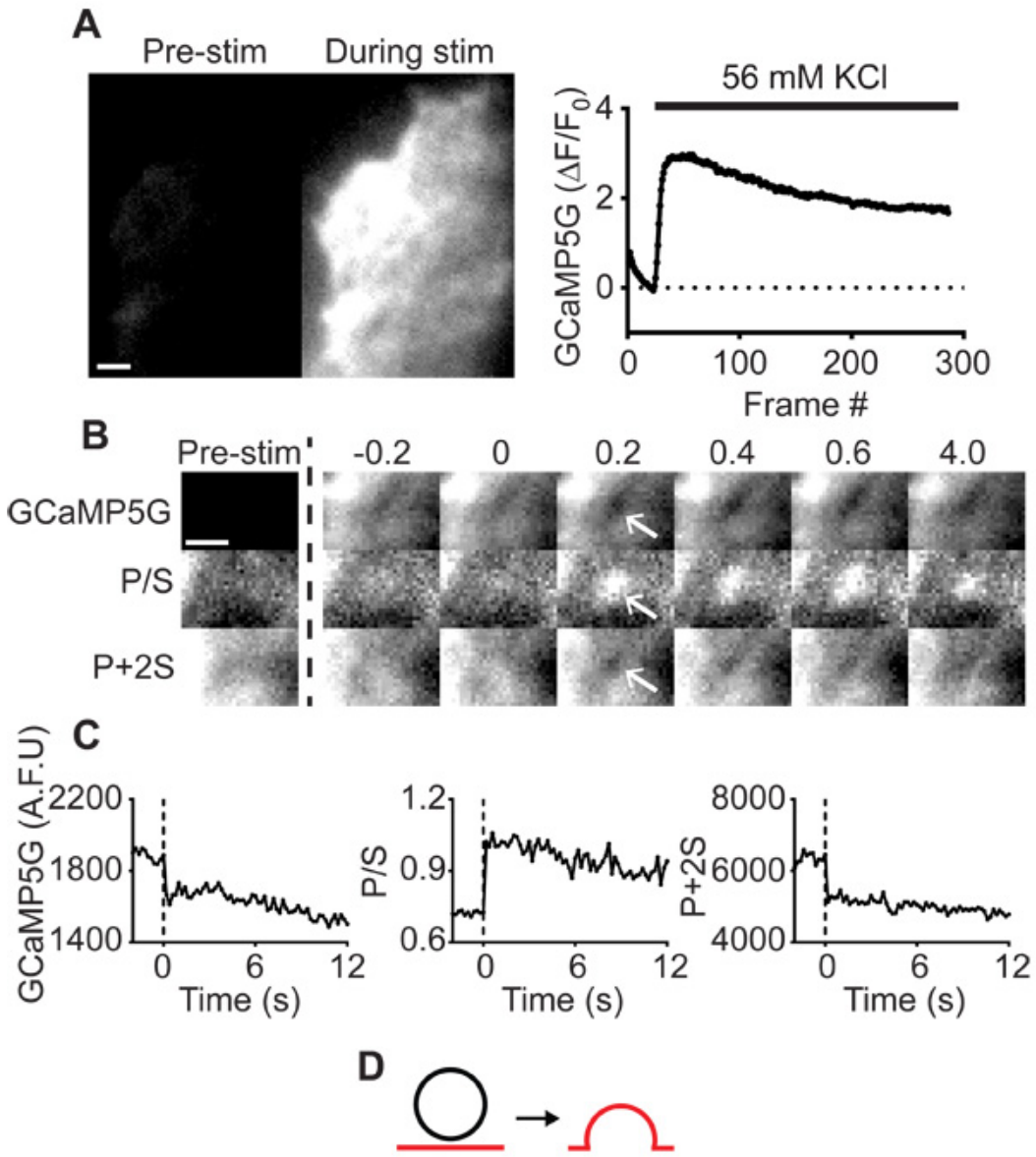


**Figure 3. Deformations are a result of stimulus-evoked $Ca^{2+}$ influx. A**) A chromaffin cell transfected with GCaMP5G is depolarized with 56 mM KCl. The resulting increase in GCaMP5G fluorescence signifies an increase in subplasmalemmal $Ca^{2+}$ levels. **B**) Frame-by-frame images of 30 x 20 pixel area of cell in A. Times above images are in seconds. White arrowheads indicate a region of P/S increase and P+2S decrease. Cytosolic GCaMP5G protein is excluded from the region by the fusing DCV. Scale bar, 1 µm. **C**) Graphs for images shown in **B. D**) One possible interpretation of the results in **B** and **C** is shown. Please click here to view a larger version of this figure.

| | | | |
|---|---|---|---|
| iXon3 EMMCD Camera | Andor | 897 | |
| IX81 Inverted Microscope | Olympus | | Side-mounted Filtercube Assembly |
| 43 Series Ar-Ion Laser | CVI Milles Griot Laser Optics | 543-AP-A01 | Tunable to 488 nm |
| Sapphire 561 LP Diode Laser | Coherent | | 561 nm |
| Scanning Galvo Mirror System | Thorlabs | GVS102 | |
| $VC^3$ Channel Focal Perfusion System | ALA Scientific Instruments | ALA VC3X4PP | |
| QMM Quartz MicroManifold | ALA Scientific Instruments | ALA QMM-4 | |
| 10 psi Pressure Regulator | ALA Scientific Instruments | ALA PR10 | |
| Manipulator | Burleigh | TS 5000-150 | |

| | | | |
|---|---|---|---|
| Mounted Achromatic Quarter-Wave Plate | Thorlabs | AQWP05M-600 | |
| 420-680 nm Polarizing Beamsplitter Cube | Thorlabs | PBS201 | |
| Six Station Neutral Density Wheel | Thorlabs | FW1AND | |
| Stepper-motor Driven SmartShutter | Sutter Instruments | IQ25-1219 | |
| HQ412lp Dichroic Filter | Chroma | NC255583 | Joins 488 nm and 561 nm beams |
| Coated Plano-Concave Lens | Edmund Optics | PCV 100mm VIS 0 | Diverges 488 nm beam |
| Coated Plano-Concave Lens | Edmund Optics | PCV 250mm VIS 0 | Diverges 561 nm beam |
| Coated Plano-Convex Lens | Edmund Optics | PCX 125mm VIS 0 | Focuses both beams |
| Coated Plano-Convex Lens | Edmund Optics | PCX 50mm VIS 0 | Cemented to filter cube assembly |
| z488/561rpc Dichroic | Chroma | z488/561rpc | Filtercube dichroic |
| z488/561_TIRF Emission Filter | Chroma | z488/561m_TIRF | Filtercube emission |
| UIS2 60X Objective | Olympus | UPLSAPO 60XO | NA 1.37 |
| Neon Transfection System | Invitrogen | MPK 5000 | |
| MetaMorph Imaging Software | Molecular Devices | | |
| DiI Membrane Dye | Invitrogen | V-22885 | For Alignment Purposes |
| TH Liberase | Roche | 5401135001 | |
| TL Liberse | Roche | 5401020001 | |
| DNAse I Type IV from bovine | Sigma | D5025 | |
| Hemocytometer | Fisher | 0267110 | |
| DiD Membrane Dye | Invitrogen | D-7757 | |
| Rhodamine | Invitrogen | R634 | |
| 0.22 µm Membrane Syringe Filter Unit | Millipore | SLGS033SS | |
| Fluoresbrite Polychromatic Red Microspheres | Polysciences | 19507 | 0.5 µm |
| Immersion Oil | Sigma | 56822 | |
| LabVIEW | National Instruments | | Controls galvo mirrors |
| Spinner Flask | Bellco | 1965-00250 | |

**Table 1. pTIRF Microscopy equipment.**

| **Contents** | **Prep-PSS** | **Basal-PSS** | **Stim-PSS** |
|---|---|---|---|
| NaCl | 145 mM | 145 mM | 95 mM |
| KCl | 5.6 mM | 5.6 mM | 56 mM |
| $MgCl_2$ | - | 0.5 mM | 0.5 mM |
| $CaCl_2$ | - | 2.2 mM | 5 mM |
| HEPES | 15 mM | 15 mM | 15 mM |
| pH | 7.4 | 7.4 | 7.4 |
| Glucose | 2.8 mM | 5.6 mM | 5.6 mM |
| Pen-Strep | 1x | - | - |

**Table 2. Perfusion and chromaffin cell prep solutions.**

| **Contents** | **Electroporating Media** | **Normal Plating Media** | **2x Antibiotic Media** |
|---|---|---|---|
| 1x DMEM/F-12 | 1 ml/plate | 2 ml/plate | 1 ml/plate |
| FBS | 10% | 10% | 10% |
| Cytosine Arabinofuranoside (CAF) | - | 1 µl/ml from 10 mM Stock | - |

| | | | |
|---|---|---|---|
| Penicillin | - | 100 units/ml | 200 units/ml |
| Streptomycin | - | 100 µg/ml | 200 µg/ml |
| Gentamycin | - | 25 µg/ml | 50 µg/ml |

**Table 3. Chromaffin Cell Media.**

| Contents | TH-PSS | TL-PSS |
|---|---|---|
| Liberase TH | 2 ml | - |
| Liberase TL | - | 0.85 ml |
| Prep-PSS | 98.0 ml | 84.0 ml |
| DNase | 8.75 mg | 7.4 mg |

**Table 4. TH-PSS and TL-PSS Solutions.**

## Discussion

Polarization-based TIRFM detects rapid, submicroscopic changes in membrane topology. Implementing the technique is relatively straightforward, particularly if TIRF optics are already in place. All that is needed is a quarter-wave plate, two polarizing cubes, and shutters to separate p-pol and s-pol illumination paths. The precise position of these components on the table is usually dictated by space available.

In order to obtain membrane topological information, the fluorescent probe used should intercalate with a fixed or known orientation. The technique, as described in this article, assumes the use of carbocyanine dyes but other dyes, such as FM1-43[14], may also be used. The membrane staining procedure itself is straightforward. Cultured cells require only a very brief exposure (less than 10 sec) to a small quantity of dil/diD to obtain exuberant labeling of the membrane. Adding excess dye leads to light scattering aggregates on the glass which diminish image quality. Over-incubating cells with dye leads to dye internalization which has detrimental effects on image quality and possibly cell viability. If a cell is stained well, there will be clear distinction in the P and S emission images. As shown in **Figure 2A**, the P emission will vividly highlight areas of the membrane that are coverslip oblique (*i.e.* the edges of the cell footprint) while the S emission intensity will be roughly uniform over the cell footprint. If a clear distinction between P and S is not apparent, then it is possible that the cell is poorly adhered to the substrate or the cell membrane is not healthy, and the cell is not used for experiments.

Our previous studies describing pTIRFM utilized dil as the fluorescent membrane probe. Here, we utilize diD because it is suitable for dual-color imaging experiments that employ GFP/pHluorin as the other fluorophore. We excite diD with a 561 nm laser rather than 640 nm laser (which is closer to its excitation peak) because the fluorophore bleaches more rapidly at 640 nm. Despite the fact that the 561 nm laser is on the tail of diD's published excitation spectrum, fluorescence is efficiently emitted. Another advantage of the 561 nm laser is that it excites both dil and diD enabling us to use the same polarization setup for both probes. Note that the orientation of the fluorophore in the membrane will affect the interpretation of membrane topology. For example, if a fluorophore were oriented with its transition dipoles perpendicular to the membrane plane (rather than parallel, or nearly parallel, as is the case with dil or diD), then nonplanar membrane regions will be more readily highlighted by the S rather than the P emission.

We have also described techniques for isolation and electroporation of bovine adrenal chromaffin cells. The bovine chromaffin cell is an excellent secretory model. It has the advantages of being easy to maintain in culture, responsive to a variety of secretogogues, and possessing large secretory vesicles that are readily visualized with conventional light microscopy. To express fluorescent proteins, cells are electroporated in suspension prior to plating on collagen-treated culture dishes. In our experience, expression efficiency is much higher with electroporation than with either $Ca^{2+}$-phosphate or Lipofectamine reagents. The drawback of electroporation is that it requires more cells (as many do not survive the process) and expensive commercial reagents. For reasons that are unclear to us, not every membrane incorporates diD. In addition, only a fraction of the cells on the dish are transfected. Finding cells that are transfected AND are stained well with diD can be time consuming which is why optimizing conditions for staining and electroporation is well worth the effort.

In summary, this article describes how pTIRFM is implemented to monitor the rapid and localized membrane deformations that occur during fusion of dense core vesicles in bovine chromaffin cells. Although only one application is discussed, the technique is ideally suited for the study of other biological processes that involve changes in membrane shape, including endocytosis, cytokinesis, and cell motility.

## Disclosures

The authors have nothing to disclose.

## Acknowledgements

This research is supported by a National Scientist Development Grant (13SDG14420049) to AA from the American Heart Association and start-up funds from Wayne State University. We are indebted to Dr. Ronald W. Holz and Dr. Mary Bittner for providing advice regarding the bovine adrenal preparations and Dr. Daniel Axelrod for assistance with the pTIRFM set-up and helpful comments on the manuscript. Syt-1 pHluorin was used with permission of Dr. Gero Miesenbock (University of Oxford). GCAMP5G was obtained through Addgene. We thank James T. Taylor, Tejeshwar Rao, Rachel L. Aikman, and Praneeth Katrapti with help on optimizing various steps of the procedures described.

## References


1. Chernomordik, L. V., Zimmerberg, J. & Kozlov, M. M. Membranes of the world unite! *J. Cell Biol*. **175**, 201-207 (2006).
2. Chapman, E. R. How does synaptotagmin trigger neurotransmitter release? *Annu. Rev. Biochem*. **77**, 615-641, doi:10.1146/annurev.biochem.77.062005.101135 (2008).
3. Hinshaw, J. E. Dynamin and its role in membrane fission. *Annu. Rev. Cell Dev. Biol*. **16**, 483-519, doi:10.1146/annurev.cellbio.16.1.483 (2000).
4. Lang, T. *et al.* $Ca^{2+}$-triggered peptide secretion in single cells imaged with green fluorescent protein and evanescent-wave microscopy. *Neuron*. **18(6)**, 857-863 (1997).
5. Steyer, J. A., Horstman, H. & Almers, W. Transport, docking and exocytosis of single secretory granules in live chromaffin cells. *Nature*. **388**, 474-478 (1997).
6. Allersma, M. W., Wang, L., Axelrod, D. & Holz, R. W. Visualization of regulated exocytosis with a granule-membrane probe using total internal reflection microscopy. *Mol. Biol. Cell*. **15**, 4658-4668 (2004).
7. Toomre, D., Steyer, J. A., Keller, P., Almers, W. & Simons, K. Fusion of constitutive membrane traffic with the cell surface observed by evanescent wave microscopy. *J. Cell Biol*. **149**, 33-40 (2000).
8. Schmoranzer, J., Goulian, M., Axelrod, D. & Simon, S. M. Imaging constitutive exocytosis with total internal reflection fluorescence microscopy. *J. Cell Biol*. **149**, 23-32 (2000).
9. Heinemann, C., Chow, R. H., Neher, E. & Zucker, R. S. Kinetics of the secretory response in bovine chromaffin cells following flash photolysis of caged $Ca^{2+}$. *Biophys. J*. **67**, 2546-2557, doi:10.1016/S0006-3495(94)80744-1 (1994).
10. Heidelberger, R., Heinemann, C., Neher, E. & Matthews, G. Calcium dependence of the rate of exocytosis in a synaptic terminal. *Nature*. **371**(6497), 513-515 (1994).
11. Chow, R. H., Klingauf, J., Heinemann, C., Zucker, R. S. & Neher, E. Mechanisms determining the time course of secretion in neuroendocrine cells. *Neuron*. **16**, 369-376 (1996).
12. Thompson, N. L., McConnell, H. M. & Burhardt, T. P. Order in supported phospholipid monolayers detected by the dichroism of fluorescence excited with polarized evanescent illumination. *Biophys. J*. **46**, 739-747, doi:10.1016/S0006-3495(84)84072-2 (1984).
13. Sund, S. E., Swanson, J. A. & Axelrod, D. Cell membrane orientation visualized by polarized total internal reflection fluorescence. *Biophys. J.* **77**, 2266-2283 (1999).
14. Zenisek, D., Steyer, J. A., Feldman, M. E. & Almers, W. A membrane marker leaves synaptic vesicles in milliseconds after exocytosis in retinal bipolar cells. *Neuron.* **35**, 1085-1097 (2002).
15. Anantharam, A., Axelrod, D. & Holz, R. W. Real-time imaging of plasma membrane deformations reveals pre-fusion membrane curvature changes and a role for dynamin in the regulation of fusion pore expansion. *J. Neurochem*. doi:10.1111/j.1471-4159.2012.07816.x (2012).
16. Anantharam, A. *et al.* A new role for the dynamin GTPase in the regulation of fusion pore expansion. *Mol. Biol. Cell*. **22**, 1907-1918, doi:10.1091/mbc.E11-02-0101 (2011).
17. Anantharam, A., Axelrod, D. & Holz, R. W. Polarized TIRFM reveals changes in plasma membrane topology before and during granule fusion. *Cell Mol. Neurobiol*. **30**, 1343-1349, doi:10.1007/s10571-010-9590-0 (2010).
18. Anantharam, A., Onoa, B., Edwards, R. H., Holz, R. W. & Axelrod, D. Localized topological changes of the plasma membrane upon exocytosis visualized by polarized TIRFM. *J. Cell Biol*. **188**, 415-428, doi:10.1083/jcb.200908010 (2010).
19. Wick, P. W., Senter, R. A., Parsels, L. A. & Holz, R. W. Transient transfection studies of secretion in bovine chromaffin cells and PC12 cells: generation of kainate-sensitive chromaffin cells. *J. Biol. Chem*. **268**, 10983-10989 (1993).
20. O'Connor, D. T. *et al*. Primary culture of bovine chromaffin cells. *Nat. Protoc*. **2**, 1248-1253, doi:10.1038/nprot.2007.136 (2007).
21. Nakai, J., Ohkura, M. & Imoto, K. A high signal-to-noise $Ca^{2+}$ probe composed of a single green fluorescent protein. *Nat. Biotechnol*. **19**, 137-141, doi:10.1038/84397 (2001).
22. Akerboom, J. *et al.* Optimization of a GCaMP calcium indicator for neural activity imaging. *J. Neurosci*. **32**, 13819-13840, doi:10.1523/JNEUROSCI.2601-12.2012 (2012).